JOURNAL OF CATALYSIS 36, 125–141 (1975)

Hydroisomerization and Hydrocracking of Normal Pentane Over Various Mordenite Catalysts

J. A. GRAY[1] AND J. T. COBB, JR.

Department of Chemical and Petroleum Engineering, University of Pittsburgh, Pittsburgh, Pennsylvania 15261

Received January 4, 1974; revised July 30, 1974

Mordenite catalysts with various cations were prepared by a reflux ion exchange technique using chloride or nitrate salts and were tested for activity in the hydroisomerization and hydrocracking of *n*-pentane. The extent of sodium ion exchange possible followed the order

$$NH_4^+ > Ba^{2+} > Sr^{2+} > Be^{2+} > Ca^{2+} > Mg^{2+} > La^{3+}.$$

Maximum catalytic activities for H-M, Ca-M and La-M occurred at calcination temperatures of 510, 525, and 400°C, respectively. Weight loss during calcination followed the order Be > Mg > Ca > Sr > Ba indicating that the smaller cation mordenites can accommodate more adsorbed water.

Increasing degrees of Na^+ ion exchange in H-M, Ca-M, Sr-M, and Ba-M resulted in increased *n*-pentane hydroisomerization and hydrocracking activity. The activity increase was small for Sr-M and Ba-M and for H-M with less than 80% exchange. Activity increased very rapidly beyond 80% exchange for H-M and appeared to increase substantially for Ca-M from 68 to 72% exchange.

Although conversion was low for Be, Mg, Ca, Sr, Ba, and La-M, the following activity order for both *n*-pentane hydroisomerization and hydrocracking was obtained:

$$Be > La > Mg > Ca > Sr > Ba.$$

The cracked products consisted of relatively more propane and butanes for the smallest cation form (Be-M) and relatively more methane for the largest cation form (Ba-M), indicating a selectivity effect. A constant effect of cation size for the alkaline earth group catalysts was evident from the Arrhenius plots, and a simple factor for cation size was introduced into the equation for the apparent rate constant so that a single Arrhenius line was obtained.

Addition of nickel to the above catalysts increased activity substantially, especially for hydrocracking. Very high hydrocracking conversions over Be, Mg, Ca, Sr, Ba, and La-M were obtained at temperatures between 370 and 480°C at a WHSV of 23.0 g/h-g. The relative order of enhancement by adding nickel was Ba > Sr > Ca > La > Mg > Be. The catalysts containing nickel produced relatively more butanes and propane and less methane than the same catalysts without nickel. The average activation energies for hydroisomerization and hydrocracking were 20.1 and 22.9 kcal/g-mole, respectively, without nickel and were 41.2 and 46.4 kcal/g-mole, respectively, with nickel.

Be-M and La-M gave peculiar Arrhenius plots which could not be explained with existing data.

NOMENCLATURE

A	constant in general Arrhenius equation
A_1	normal paraffin molecule or frequency constant in Arrhenius equation for hydroisomerization
A_2	iso-paraffin molecule

[1] Present address: U. S. Bureau of Mines, Pittsburgh Energy Research Center, Pittsburgh, PA.

Copyright © 1975 by Academic Press, Inc. All rights of reproduction in any form reserved.
Printed in the United States.

A_c frequency constant in Arrhenius equation for hydrocracking
A_r reactor cross-sectional area, cm^2
B constant in general Arrhenius equation
C total molar gas concentration, g-mole/cm^3
E_1 activation energy for hydroisomerization
E_c activation energy for hydrocracking
F total molar feed rate, lb-mole/h
K hydroisomerization equilibrium constant
R gas law constant
S_g catalyst specific surface area, m^2/g
$S_g k_1$ hydroisomerization apparent reaction rate constant, cm^3/h-g
$S_g k_c$ hydrocracking apparent reaction rate constant, cm^3/h-g
T temperature
W_c catalyst weight, g
Z axial coordinate for reactor, cm
a_i mole fraction of component i
a_{i0} initial mole fraction of component i
a_{iL} final mole fraction of component i
k_1 hydroisomerization forward reaction rate constant, cm^3/h-cm^2
k_2 hydroisomerization reverse reaction rate constant, cm^3/h-cm^2
k_1' hydroisomerization apparent reaction rate constant, independent of cation size, cm^3/h-g
k_c hydrocracking reaction rate constant, cm^3/h-cm^2
k_c' hydrocracking apparent reaction rate constant independent of cation size, cm^3/h-g
n hydrogen stoichiometric coefficient
r_c cation radius, Å
α constant defined by $\gamma = A_r \rho_b S_g C/F$
γ initial molar ratio of hydrogen to hydrocarbons
ρ_b catalyst bulk density, g/cm^3
2σ 95% confidence limits
φ_1 cation radius coefficient for hydroisomerization Å^{-1}
φ_c cation radius coefficient for hydrocracking Å^{-1}
Ψ_1 hydroisomerization activity of nickel catalyst relative to same catalyst without nickel
ψ_c hydrocracking activity of nickel catalyst relative to same catalyst without nickel

INTRODUCTION

The active sites in various mordenite catalysts have been investigated to some extent (*1–7*) and appear similar to those in the synthetic faujasite counterpart. Despite this similarity, however, mordenite has its own peculiar properties. Steric effects on conversion and selectivity are very pronounced because of the smaller pore size in comparison with Type Y zeolite (*6–10*). Unlike typical bifunctional catalysts, H–M (with or without a Group VIII metal component) is active for isomerization of paraffins and cycloparaffins but not also dehydrogenation of them (*11,12*). Addition of Ni, Pd, or Pt to H–M does not increase its *n*-pentane or *n*-hexane isomerization activity as with H–Y zeolite (*11–16*). Alkaline earth and alkali metal cation mordenites are very active for benzene hydrogenation in the absence of a Group VIII metal component, but are not very active in cyclohexane isomerization (*11,12*).

Although many different cation forms of mordenite catalysts have been reported (*6,8,11,12*), a systematic study of a particular group along with complete ion exchange data has not been presented. Little is mentioned in the literature concerning the effect of pretreatment temperature (*1,2,7*) and the degree of exchange (*11,12*) on mordenite catalysts. Very little attention has been given to alkaline earth mordenites containing a Group VIII metal component. This paper will report on the

effects of pretreatment temperature, degree of exchange, alkaline earth cation size, and the addition of nickel on mordenite catalyst activity. In addition, ion exchange data will be presented.

EXPERIMENTAL

Apparatus

All catalyst tests were performed in a conventional bench-scale pilot unit containing a 2.43 cm diameter, tubular, fixed-bed reactor. Details of the pilot unit are given elsewhere (*17*). The catalyst bed temperature was maintained isothermal to within 2°C in most cases and was checked by radial and axial temperature measurements. The charge was usually 15.0 g of 10/20 mesh size undiluted catalyst. With some of the nickel catalysts, temperature control was difficult and required using 3.0 g of catalyst diluted with 60.0 gms of inert quartz. The hydrogen(Linde, Prepurified Grade passed through a purifier system)-to-normal pentane (J. T. Baker Chemical Co., 99+%) molar feed ratio was about 3.5 and the reactor pressure was 31.6 atm.

Preliminary tests with H–M demonstrated that mass transfer resistance, both external and in the macro-pores of the catalysts particles, was not significant under the experimental conditions used for this work.

The hydrogen/air/methane gas chromatograph analysis was performed using a 3 mm × 5.49 m column of 50/80 mesh Porapak S at 30°C and a 20 cm^3/min carrier gas (8.5% H_2, 91.5% He) flow rate. The ethane through hexanes analysis was performed using a 6.35 mm × 9.14 m column of 27% Silicone Oil DC 200 on 60/80 mesh Chromosorb P at 90°C and a 50 cm^3/min He carrier gas flow rate. All material balances were within 98–102%.

Catalyst Preparation and Analysis

Synthetic sodium mordenite (Norton Company Zeolon 100) was used as the starting material for all catalysts and has the chemical analysis shown in Table 1. The sodium mordenite was exchanged for 2 h at reflux temperature with the appropriate salt solution. The exchanged zeolites were washed free of excess salt and dried overnight at 105°C. The exchange data are shown in Tables 2 and 3. After pressing and screening, the exchanged mordenite was calcined in a box furnace. The calcination was started at 150°C. The temperature was increased in 75°C steps every hour and was held at the desired temperature until 24 h after the starting time. Nickel catalysts were reduced with hydrogen *in situ* (400°C, 7.80 atm, 40–50 cm^3/min) in addition to calcination.

TABLE 1
SODIUM MORDENITE ANALYSIS

Wt. % SiO_2	69.01
Wt. % Al_2O_3	11.00
Wt. % Na_2O	6.45
SiO_2/Al_2O_3 (mole)	10.64
Na_2O/Al_2O_3 (mole)	0.9646

The alumina content of the exchanged mordenite was determined by one of three methods: first, by atomic absorption (*17*); second, by correcting the alumina content of the starting Na–M using ion exchange weight change data; third, by calculation using the silica analysis and the silica/alumina ratio of the starting Na–M. Silica was determined in several cases by a wet chemical technique (*18*), nickel by atomic absorption (*17*), ammonia by the Kjeldahl method, and sodium by flame emission.

Kinetic Model–Data Correlation

A detailed mechanism is not given but rather the Langmuir adsorption terms are left imbedded in the apparent reaction rate constants. Based on the previous work with pentane, hexane, and cyclohexane (*13,14,17,19–21*), this type of approach is valid only if total pressure is held constant. The following reaction scheme is used:

TABLE 2
ION EXCHANGE DATA

Catalyst	Salt solution normality	No. of times exchanged	Wt. % Na_2O	Wt. % Al_2O_3	% Exchange
NH_4-M	1.305	1	0.462	11.48	93.4
NH_4-M	1.305	1	0.474	11.33	93.1
NH_4-M	1.305	1	–	–	93.2
NH_4-M	1.185	2	0.0567	11.71	99.2
NH_4-M	0.624	1	0.862	11.48	87.6
NH_4-M	0.474	1	1.12	11.47	83.9
NH_4-M	0.237	1	2.30	11.35	66.7
Be-M	1.185	2	2.06	10.90	68.9
Be-M	1.185	2	2.09	11.09	69.0
Mg-M	1.185	3	2.46	11.28	64.1
Ca-M	1.185	3	1.84	10.67	71.6
Ca-M	1.185	2	2.18	11.10	67.7
Sr-M	1.185	3	1.02	10.68	84.3
Sr-M	1.185	1	2.35	10.66	63.7
Ba-M	1.185	3	0.650	10.53	89.8
Ba-M	0.711	1	2.00	10.31	68.1
La-M	0.711	2	2.54	10.70	60.9
La-M	0.711	2	2.50	10.61	61.2

Chloride salts used except for Be-M and Mg-M for which nitrate salts used. Starting Na-M weight/solution volume ratio is 114 g/liter.

TABLE 3
NICKEL ION EXCHANGE RESULTS

Catalyst	Wt. % Na_2O	Wt. % Ni	Wt. % Al_2O_3	% Na sites	% Ni sites	% Other sites	Δ% Other sites	Δ% Na sites
Ni-Be-M	1.83	0.796	10.82	27.8	12.8	59.4	−9.5	−3.3
Ni-Mg-M	2.34	0.823	11.19	34.4	12.8	52.8	−11.3	−1.5
Ni--Ca-M	2.00	0.760	11.00	29.9	12.0	58.1	−9.6	−2.4
Ni-Sr-M	1.74	1.17	10.64	26.9	19.1	54.0	−9.7	−9.4
Ni-Ba-M	1.40	1.23	10.34	22.3	20.7	57.0	−11.1	−9.6
Ni-La-M	2.23	0.288	10.62	34.5	4.7	60.8	−0.4	−4.3

Exchanged once with 1 liter of $Ni(NO_3)_2 \cdot 6H_2O$ solution. Ni/Na equivalent ratio (exchange solution/mordenite) = 5/1.

$$\begin{array}{ccc} A_1 & \underset{k_2}{\overset{k_1}{\rightleftharpoons}} & A_2 \\ +nH_2 & & +nH_2 \\ & {\scriptstyle k_c}\searrow \quad \swarrow{\scriptstyle k_c} & \\ & (n+1)A_3 & \end{array} \qquad (1)$$

where the moles of various cracked products are lumped together as A_3. A_1 and A_2 are *n*-pentane and isopentane, respectively, and $(n + 1)$ is the stoichiometric coefficient for the cracked products. The total moles (hydrogen + hydrocarbons) are assumed conserved since only paraffin molecules appeared to be formed in this work. The hydrocracking rate is assumed independent of the hydrogen concentration since excess hydrogen is always present. Assuming the reactor is isothermal and plug flow exists, the reaction rate expressions,

$$da_1/dz = \alpha[-(k_1 + k_c)a_1 + k_2 a_2], \qquad (2)$$

$$\frac{da_2}{dz} = \alpha[k_1 a_1 - (k_2 + k_c)a_2], \quad (3)$$

$$\frac{da_3}{dz} = \alpha(n+1)k_c(a_1 + a_2) \quad (4)$$

are easily integrated and solved for the following apparent rate constants:

$$S_g k_c = -\frac{F}{W_c C} \ln\left[1 - \frac{a_{3L}(\gamma+1)}{(n+1)}\right], \quad (5)$$

$$S_g k = -\frac{F}{W_c(1 + 1/K)C}$$

$$\ln\left[\frac{1 - \dfrac{(\gamma+1)(1+1/K)a_{2L}}{1-(\gamma+1)/(n+1)a_{3L}}}{1-(\gamma+1)(1+1/K)a_{20}}\right]. \quad (6)$$

By evaluating Eqs. (5) and (6) for each mordenite catalyst, a comparison of catalyst activity can be made even though the data may have been obtained at various conditions (pressure always 31.6 atm). This model has been verified for H–M (*13,14,17,19,21*) and was assumed valid for the other mordenite catalysts.

RESULTS

Ion Exchange Results

Except for Be, the completeness of exchange for the alkaline earth group cations increases as the size of the cation increases (Fig. 1). The beryllium cation is very small compared to the other cations in the alkaline earth group, and consequently possesses a very high charge density. This high charge density causes the Be^{2+} ion to be heavily hydrated, much more so than Mg^{2+} (*22*). Thus, the hydrated beryllium cation is larger than 0.35 Å, has a more diffuse charge density, and consequently has an ion exchange capacity between calcium and strontium, i.e., Ba > Sr > Be > Ca > Mg. Similar interactions have been observed for ion exchange resins and solvents. For example, on a sulphonic acid cation-exchange resin, the ion selectivity order is Ba > Sr > Ca > Be > Mg (*22*).

Beyond three batch exchanges, the exchange curves in Fig. 1 begin to level off. Another author used a 10/1 initial ratio of exchanging cation equivalents to sodium ion equivalents (5/1 ratio used in this work) and after three batch exchanges obtained 65.7 and 76.2% exchange for magnesium and calcium, respectively (*8*). These numbers appear to be limits of exchange and agree well with the curves of Fig. 1. In other published work, 100% exchange was achieved for calcium when the exchanging salt was calcium acetate (*5*). Apparently ammonium mordenite was the starting material. Higher exchanges have been reported for magnesium (84%) and calcium (85%) (*3,6*).

For ammonium ion exchange, a complete exchange for the sodium ions is possible. In Fig. 2 the relationship between percent exchange and the ratio of the initial moles of NH_4^+ ions in the salt solution to the initial moles of Na^+ ions in the sodium mordenite is shown. The curve increases rapidly up to a ratio of 2 and then asymptotically approaches 100% at higher ratios. It seems the exchange up to about 84% corresponds to sodium replacement in easily accessible locations. Beyond 84%, less accessible sites are selectively filled by ammonium ions.

In the nickel ion exchanges shown in Table 3, the number of alkaline earth cat-

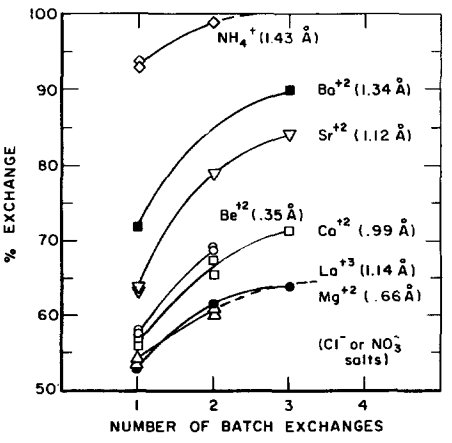

FIG. 1. Percent exchange vs number of exchanges.

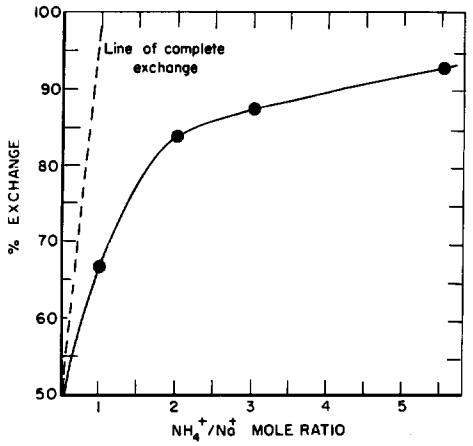

FIG. 2. Percent exchange vs NH_4^+/Na^+ mole ratio.

ions replaced by Ni^{2+} ions varied randomly from 9.5 to 11.3% and averaged about 10%. However, the decrease in the number of sodium ions during nickel exchange was not random and followed the order Ba > Sr > Be > Ca > Mg. Apparently, the alkaline earth cations affect the number of sodium ions which can be replaced by Ni^{2+} ions in parallel with the size selectivity for alkaline earth cations. This may have been caused by not keeping constant the equivalents of exchanging nickel. Instead, the equivalents ratio of nickel to sodium was kept at 5/1, where the % Na sites varied from 31.0 to 36.3% before nickel exchange.

When nickel was exchanged into the lanthanum mordenite, practically none of the lanthanum was lost. The small amount of exchange which occurred involved, almost exclusively, the sodium cations.

Pretreatment Temperature

Hydrogen, calcium, and lanthanum mordenite catalysts were calcined at various temperatures from 400 to 650°C. As shown in Fig. 3, the total pentane conversion (hydrocracking plus hydroisomerization) for all three catalysts reached a maximum at about 500–525°C. The calcium and lanthanum mordenite catalysts had low activity and consequently did not show as dramatic an effect as the hydrogen mordenite catalyst. The hydrogen mordenite catalyst was so sensitive that increasing the calcination temperature from 400 to 510°C changed the total conversion from 11.5 to 63%. Increasing the calcination temperature about another 90°C caused a rapid decrease in conversion to about 12%.

Figure 4 illustrates the effect of the calcination temperature on the individual hydroisomerization and hydrocracking reactions. The apparent rate constants for H–M behave the same as the total conversion curve in Fig. 3, yielding maxima at 510°C. The Ca–M and La–M catalysts were more active for hydrocracking than for hydroisomerization and yielded optimum values of the apparent rate constants at 525 and 400°C, respectively for the latter reaction. The hydrocracking reaction was not sensitive to calcination temperature beyond 500°C for Ca–M and appeared unaffected over the entire experimental range for La–M. These results suggest that hydroisomerization activity is associated with Bronsted acid site (hydroxyl group) concentration which reaches

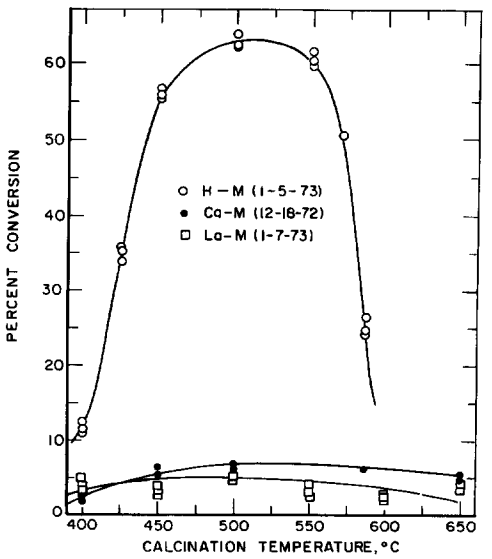

FIG. 3. Percent conversion vs calcination temperature.

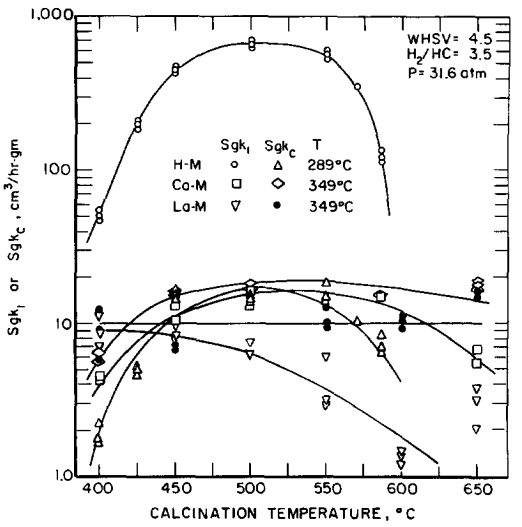

FIG. 4. Apparent reaction rate constant vs calcination temperature.

a maximum at an optimum calcination temperature. The insensitivity of the hydrocracking reaction to pretreatment temperature for the Ca–M and La–M catalysts may have resulted because all proton sites did not take part in the catalysis and loss of some of these sites through dehydroxylation had little effect. A similar effect has been observed with isooctane cracking over a La–Y catalyst (*23*). Some hydroxyl groups were probably introduced by hydrogen-ion exchange during treatment of the mordenite with the acidic lanthanum salt solution (*24*). However, the influence of these groups on hydroisomerization and hydrocracking activity is believed to be minimal because the optimal pretreatment temperature and hydrocracking responses to pretreatment temperature are quite different for H–M, having a large number of hydroxyl groups, and La–M. The cracked product distribution for the La–M catalyst in activity tests at 350°C and 31.6 atm seemed to indicate an ionic mechanism was operative. The moles of ethane and propane were about equal and isobutane represented a significant amount of the butanes yield. The isobutane/*n*-butane ratio decreased with calcination temperatures above 400°C in the same fashion as the isopentane yield. The relatively large yield of methane in comparison to the other cracked products suggests that a radical mechanism may have also been in effect and could become more significant at higher reaction temperatures (*25,26*). The optimum pretreatment temperature for the NH_4–M, Ca–M, and La–M catalysts are different from each other because each cation creates distinct and independent acid sites during dehydration (and deammination for NH_4–M) (*27,28*).

The calcination temperature at which maximum conversion occurred over the H–M catalyst (510°C) does not agree with either of two temperatures already reported. One author (*7*) obtained the maximum at 450°C for benzene alkylation and the other author (*1*) found the maximum at 675–700°C for toluene disproportionation and normal paraffin (pentane and butane) isomerization and cracking. This discrepancy is not due to Si/Al ratio because this factor was almost the same for the previous authors (7.35 vs 7.03). The degree of exchange is not an influencing factor either since H–$M^{675-700}$ was 99.7% exchanged, and H–M^{510} of this work was 99.2% exchanged. Even though all the above reactions were carbonium-ion type and were strongly influenced by hydroxyl group (Bronsted acid sites) concentration, the differences in optimum pretreatment temperature can be attributed to either the reaction used, the reaction conditions, or differences in pretreatment. The only common reaction was pentane conversion for H–M^{510} and H–$M^{675-700}$. However, the reaction conditions were different since the reactor atmosphere was hydrogen for H–M^{510} and helium for H–$M^{675-700}$. A hydrogen atmosphere, for example, was shown to considerably enhance cracking activity (*29*). One author (*23*) has pointed out that even for the same reaction various responses to pretreatment temperature can be observed depending on the experi-

mental conditions and differences in the nature of the active sites. The method of calcination was greatly different for the three H–M catalysts indicating that ammonia removal caused some differences. For H–M^{450}, the reactor was evacuated during a 30 min calcination. The H–$M^{675-700}$ catalyst was calcined for 30 min in a helium gas stream. The H–M^{510} catalyst of this work was calcined for 24 hr in air. Thus, the lower optimum pretreatment temperature for H–M^{510} as compared to H–$M^{675-700}$ can be at least partially attributed to the longer activation time (*2*) and the presence of oxygen in the calcining atmosphere (*28*). Both longer activation times and an oxygen atmosphere lower the optimum activation temperature. The lower optimum pretreatment temperature of the H–M^{450} catalyst probably resulted from evacuation during pretreatment and the different reaction used to measure catalytic activity.

Weight loss data at 500°C is presented in Fig. 5 for the alkaline earth mordenite catalysts with and without nickel. In both cases, the amount of water loss during calcination decreased as cation size increased. This was expected since the volume available for adsorbed water decreases as the cation size increases. This is in agreement with data for Type Y Zeolite (*30*).

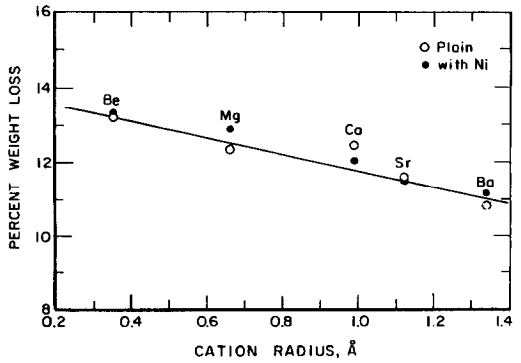

FIG. 5. Percent weight loss at 500°C vs cation radius-alkaline earth group.

Degree of Sodium Replacement

The degree of sodium replacement in mordenite catalysts affected activity in a way similar to the synthetic faujasite catalysts. Figure 6 illustrates some conversion data for hydrogen mordenite and three alkaline earth mordenites. In the case of H–M, *n*-pentane conversion increased slowly with increased degree of sodium replacement until about 80% exchange. Beyond 80% exchange the conversion increased very rapidly at a linear rate. The effect on hydroisomerization and hydrocracking individually is shown in Fig. 7. This very same effect of exchange degree has been observed for H–Y zeolite (*31*). Apparently the last few percent of sodium ions either occupy the active sites or somehow directly affect these sites. Since the cation locations in mordenite are not fully known, it is difficult to say just what these last few sodium ions do or where they are located. This scheme also agrees with the ion exchange behavior exhibited in Fig. 2, where sodium replacement was rapid up to about 80% and the remaining sodium became more difficult to displace.

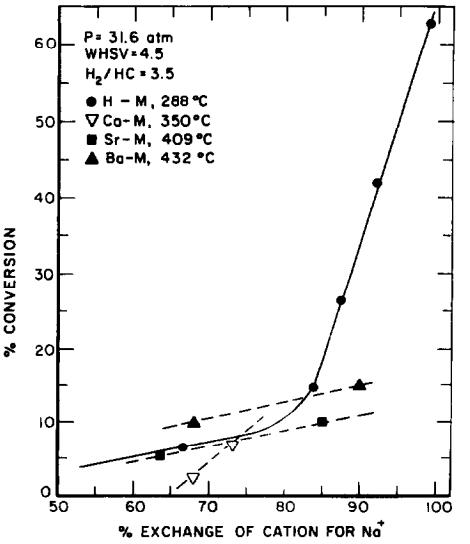

FIG. 6. Percent conversion vs percent exchange of cation for Na^+.

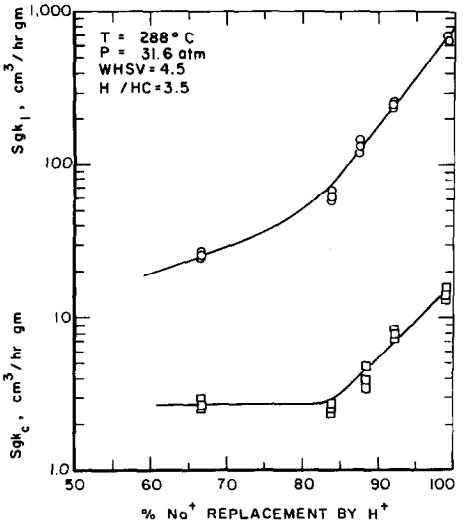

FIG. 7. Apparent reaction rate constant vs percent Na^+ replacement by H^+.

In contrast to these results, another author (*11*) observed that cyclohexane isomerization on mordenite increased at an almost uniform rate with increasing replacement of sodium by hydrogen. Thus, the reaction by which activity is measured is important and can yield different responses to sodium replacement. Similar differences can be found in the literature for H–Y zeolite. Cumene cracking (*31*) for instance will give different responses to sodium replacement than 0-xylene isomerization (*32*) or dehydration of 1-pentanol (*11*). The basic characteristic of these responses stays the same, but the onset of rapid activity increase and the degree of rapidity of increase can vary.

The effect of degree of sodium replacement was not as pronounced in the Sr–M and Ba–M catalysts as shown in Fig. 6. The *n*-pentane conversion increased slowly with increasing degree of exchange and showed no deviation from this trend even up to 90% exchange in the case of Ba–M. The effect on the apparent reaction rates is illustrated for Ba–M in Fig. 8 as Arrhenius plots. Hydrocracking activity appears to be only slightly enhanced with degree of exchange, most of the change occurring in hydroisomerization.

Barium and strontium cations, because of their size and the smaller channel size of mordenite compared to faujasite, probably are unable to create significant acidity. The charge separation is just not adequate to create strong electrostatic fields within the channels. The low acidity and activity of a Ba–Y catalyst has already been demonstrated (*33*). Although Sr–Y was reported as acidic and active (*33*), the smaller channel structure of mordenite probably causes enough difference to make Sr–M relatively inactive. *n*-Pentane conversion for the Ca–M catalysts increased much more rapidly with increasing degree of sodium replacement than for the Sr–M and Ba–M catalysts. The calcium ion probably generates considerable acidity because of its small size and higher charge density compared to strontium and barium.

The more exchanged catalysts seem to have a lower hydroisomerization activation energy and a higher selectivity for hydroisomerization than the less exchanged catalysts. These results are shown in Table 4, where the activation energy

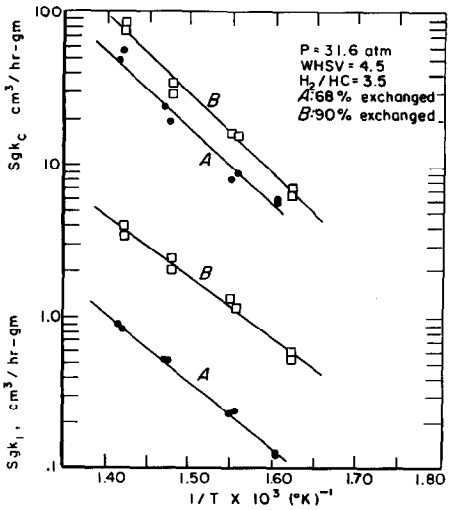

FIG. 8. Ba–M Arrhenius plot for two levels of exchange.

TABLE 4
ACTIVATION ENERGIES AND ISOMERIZATION SELECTIVITIES FOR VARIOUS LEVELS OF EXCHANGE IN ALKALINE EARTH MORDENITES

Catalyst	% Exchange	E_1 kcal/g-mole	E_c kcal/g-mole	ΔE_1 Δ% Exchange	ΔE_c Δ% Exchange	Isomerization selectivity (%)
Ca-M	68	21.31	23.27			3.7[a]
				3.47	2.88	
Ca-M	72	7.41	34.81			48.0
Sr-M	64	19.06	18.05			4.6[b]
				0.37	0.18	
Sr-M	84	11.63	21.70			7.5
Ba-M	68	20.39	23.06			1.0[c]
				0.09	0.04	
Ba-M	90	18.33	23.88			2.9

[a] 350°C.
[b] 409°C.
[c] 432°C.

decrease and selectivity increase follow the order Ca > Sr > Ba. The hydrocracking activation energy increased with increasing exchange. Thus, the hydroisomerization reaction becomes increasingly favorable at higher degrees of exchange while the hydrocracking reaction becomes less favorable. This appears to result from widening of the micro-channels so that the isopentane molecule is more easily accommodated. Although there was no apparent diffusional resistance in the macropores of the catalysts, a diffusion limitation in the micro-channels of the mordenite crystal is a valid possibility and would not be detected by conventional tests. This type of diffusion resistance would account for the differences in activation energy.

Cation Size and Charge

In order to determine the effect of cation size and charge on *n*-pentane conversion, alkaline earth and rare earth mordenite catalysts were prepared having approximately equal degrees of exchange, 64 to 69% for the former catalysts and 61% for

TABLE 5
n-PENTANE CONVERSION OVER MORDENITE CATALYSTS

Catalyst	Temp. (°C)	WHSV (g/h-gm)	% *n*-pentane hydroisomerized	% *n*-pentane hydrocracked
Be-M	345	4.5	5.65	2.73
Be-M	436	4.6	4.99	19.29
Mg-M	346	4.5	0.34	1.85
Mg-M	439	4.5	3.74	25.74
Ca-M	350	4.5	0.10	2.55
Ca-M	437	4.7	1.47	13.90
Sr-M	370	4.6	0.20	3.39
Sr-M	437	4.6	0.46	8.54
Ba-M	370	4.9	0.04	1.86
Ba-M	432	4.7	0.07	10.43
La-M	347	4.7	0.63	2.32
La-M	430	4.6	2.73	22.31

the latter catalyst. Some conversion data are presented in Table 5. These catalysts were fairly active for hydrocracking but gave low hydroisomerization conversions. Despite these low conversions, the chromatographic analysis was accurate enough to establish interesting cation effects.

The results are presented as Arrhenius plots in Figs. 9 and 10. The catalyst activity for *n*-pentane hydroisomerization and hydrocracking was in the order Be > La > Mg > Ca > Sr > Ba. This same order of activity has been demonstrated for *n*-hexane hydrocracking/hydroisomerization and cumene cracking over alkaline earth exchanged Type Y zeolite catalysts (*30*). The strontium catalyst deviated from this order at some temperatures in hydrocracking probably because of the difference in degree of exchange. The hydroisomerization activity was affected much more by cation size and charge than the hydrocracking activity. This was not unexpected since steric hindrance from cations in the mordenite channels would favor smaller product molecules. The hydrocracking reaction, unlike the hydroisomerization reaction, probably compensated somewhat for steric hindrance by forming small cracked product molecules. Examination of cracked product distributions and stoichiometric coefficients verified this hypothesis (*17*). The Be–M catalyst gave a fairly even distribution of methane, propane, and butanes. In going in order from the Be (smallest cation) to the Ba (largest cation) cation forms, the amounts of propane and butanes rapidly decreased until the Ba–M gave practically all methane. Since a relatively small amount of ethane compared to propane was formed, the pentane molecule was probably cracked in methane steps, i.e., pentane → butane → propane → ethane.

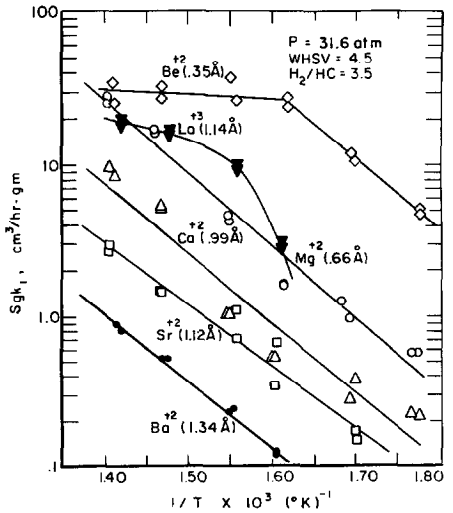

FIG. 9. Effect of cation size and charge on hydroisomerization activity.

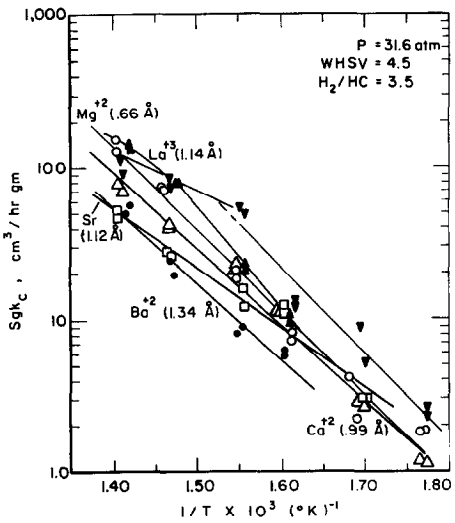

FIG. 10. Effect of cation size and charge on hydrocracking activity.

In comparing cation charge, the La^{3+} catalyst was more active than all those containing the alkaline earth cations except for Be^{2+}. The La–M catalyst activity probably would have exceeded the activity of Be–M had the degree of exchange been the same instead of 8% lower. Also, the La–M catalyst was calcined at 500°C instead of the optimum temperature of 400°C, reducing the activity by about 32%. Thus, the order of activity probably should be La > Be > Mg > Ca > Sr > Ba.

In the case of Be–M and La–M, the

apparent reaction rate constants behaved rather peculiarly with increased reaction temperature. This will be discussed after presenting the nickel catalyst results.

The activation energies for the mordenite catalysts, without and with nickel, are listed in Table 6 along with the frequency constants. The activation energies for the catalysts without nickel are low compared to those normally obtained in *n*-pentane hydroisomerization and hydrocracking. A possible reason for this will be discussed later with the nickel catalyst results.

The fact that the activation energies are approximately equal suggests that a relative activity, somewhat independent of temperature, can be calculated in order to separate out the effect of cation size. Figure 11 is the result of dividing the apparent reaction rate constant of each cation form at 288 and 344°C by the apparent reaction rate constant of Ba–M at the same temperature and plotting versus cation radius.

The relative activity of a H–M catalyst (66.7% exchanged) is included where the effective ionic radius of the proton was estimated as $1/9 \times 0.35 \times 2 = 0.078$ Å, where 1 and 9 are the atomic weights of hydrogen and beryllium, respectively, 0.35

TABLE 6
ACTIVATION ENERGIES OF MORDENITE CATALYSTS

Catalyst	E_1 (kcal/ g-mole)	E_c (kcal/ g-mole)	A_1	A_c
Be–M	20.77	25.91	20.15	23.97
Mg–M	22.00	24.96	18.77	22.51
Ca–M	21.31	23.27	17.06	20.97
Sr–M	19.06	18.05	14.58	16.71
Ba–M	20.39	23.06	14.42	20.28
Ni–Be–M	35.73	37.01	33.39	32.69
Ni–Mg–M	44.34	54.18	39.02	47.12
Ni–Ca–M	48.71	58.91	42.45	51.88
Ni–Sr–M	42.17	43.27	38.48	39.76
Ni–Ba–M	35.16	38.58	32.99	34.98
Ni–La–M	43.13	54.22	38.66	47.76

$\ln(S_g k_1) = A_1 - E_1/RT$
$\ln(S_g k_c) = A_1 - E_c/RT$

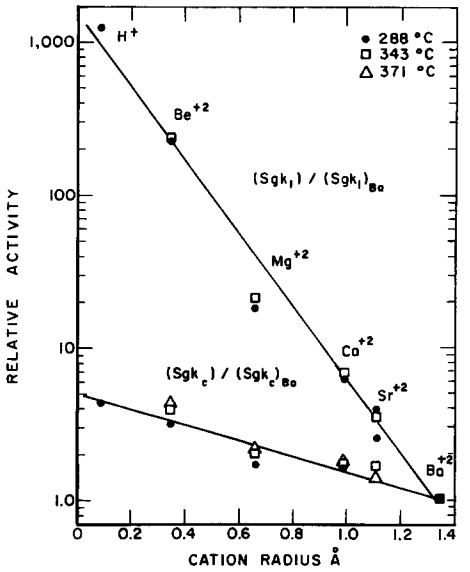

FIG. 11. Relative activity vs cation radius.

Å is the ionic radius of beryllium, and the factor 2 since there are twice as many monovalent cations. The log of relative activity varies linearly with the cation radius, both in hydroisomerization and hydrocracking, with some dependence on temperature. This result is in disagreement

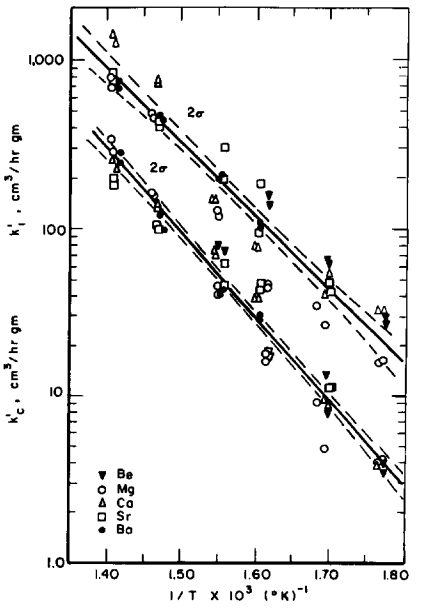

FIG. 12. Hydroisomerization and hydrocracking Arrhenius plots independent of cation size.

with previous work where ethyl alcohol was dehydrated over Mg, Ca, and Ba–M, and no correlation with cation radius was obtained (*8*). However, the same authors did find such a correlation for zeolite Type A. As sited previously, a correlation was found for zeolite Type Y in several reactions (*30*).

Based on the results of Fig. 11, it was possible to correct all the apparent reaction rate constants for the cation size effect, bringing the results together on a single Arrhenius line (Fig. 12). This was done by defining a new apparent reaction rate constant as

$$k_1' = (S_g k_1 e^{\phi_1 r_c}) = \mathrm{Be}^{-E_1/RT},$$

where r_c is the cation radius, ϕ_1 is a constant determined using Fig. 11, and B and E_1 are determined by regression analysis of the data in Figs. 9 and 10. The resulting Arrhenius equations are

$$\ln k_1' = 20.95 - \frac{20.1 \text{ kcal/g-mole}}{RT},$$

$$\ln k_c' = 20.77 - \frac{22.9 \text{ kcal/g-mole}}{RT},$$

and ϕ_1 and ϕ_c are 5.02 and 1.21, respectively. Since this analysis is rather empirical, the small effect of temperature on ϕ_1 and ϕ_c is neglected. The facts (a) that hydrocracking was not affected as dramatically as hydroisomerization with increasing cation size in the alkaline earth group catalysts, (b) that the hydrocracking reaction formed smaller product molecules with increased cation size, and (c) that the effect of cation size could be expressed as a separate entity within the equation for the apparent reaction rate constant, strongly suggest that steric hindrance of intermediate and product molecules rather than catalyst acidity is the dominant factor in alkaline earth mordenite catalysts at a constant degree of sodium exchange. Variations in degree of exchange, however, probably affect acidity as much as any steric effects.

Addition of Nickel

In order to observe the effect of a transition metal on mordenite catalyst activity, nickel catalysts were prepared from alkaline earth mordenites and lanthanum mordenite as listed previously in Table 3. Some *n*-pentane conversion data are shown in Table 7. These catalysts were very active for hydrocracking (a very exothermic reaction) and consequently made reactor temperature control difficult due to the heat removal limitation of the fixed bed. For reaction temperatures above 350–370°C all the catalysts except Ni–Be–M had to be diluted with inert quartz.

The Ni–Be–M catalyst was selective for hydroisomerization at lower temperatures and for hydrocracking at higher temperatures. The Ca, Sr, Ba, and La–M catalysts were strongly selective for hydrocracking.

The results of the nickel catalyst tests are shown as Arrhenius plots in Figs. 13 and 14. The effect of cation size was obscure in these results probably because of variations in the nickel content, location, and reducibility from one catalyst to another. The relative increase in activity can be calculated (using the results in

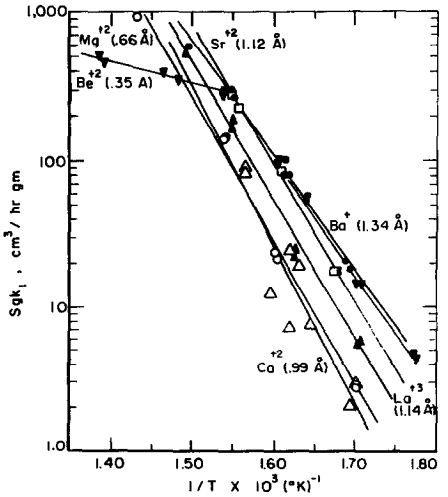

FIG. 13. Hydroisomerization Arrhenius plots for the nickel catalysts.

TABLE 7
n-PENTANE CONVERSION OVER NICKEL MORDENITE CATALYSTS

Catalyst	Temp. (°C)	WHSV (g/h-g)	% *n*-pentane hydroisomerized	% *n*-pentane hydrocracked
Ni-Be-M	349	4.7	17.0	3.2
Ni-Be-M	376	4.7	33.1	14.6
Ni-Be-M	402	4.6	29.1	30.1
Ni-Be-M	444-453[a]	4.5	10.9	76.4
Ni-Mg-M	349	4.5	4.3	4.5
Ni-Mg-M	371-409[a]	4.6	11.1	28.4
Ni-Mg-M	380-425[a]	4.6	13.0	31.5
Ni-Mg-M	375	21.4	5.1	10.2
Ni-Mg-M	425	23.1	10.0	61.9
Ni-Ca-M	353	4.6	1.7	27.4
Ni-Ca-M	343-390[a]	4.6	1.3	22.5
Ni-Ca-M	411-534[a]	4.6	2.0	80.3
Ni-Ca-M	367	23.0	3.0	10.6
Ni-Sr-M	323	4.6	3.7	5.3
Ni-Sr-M	414-549[a]	4.6	1.5	85.0
Ni-Sr-M	348	13.9	5.2	11.6
Ni-Sr-M	502-542[a]	13.8	0.9	78.5
Ni-Sr-M	373	22.7	8.9	15.6
Ni-Sr-M	406-456[a]	22.7	8.1	58.6
Ni-Sr-M	402-426	22.9	12.5	54.1
Ni-Ba-M	347	4.6	16.2	11.5
Ni-Ba-M	372	23.1	9.8	16.7
Ni-Ba-M	396	23.4	5.2	15.3
Ni-La-M	342	4.6	4.9	4.3
Ni-La-M	372	24.2	5.7	12.8
Ni-La-M	398	24.0	11.3	37.7

[a] Nonisothermal axial temperature range.

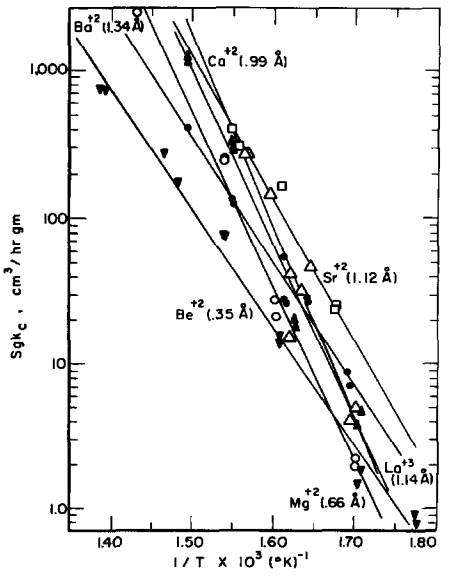

FIG. 14. Hydrocracking Arrhenius plots for the nickel catalysts.

Table 6) as the apparent rate constant of the catalyst containing nickel divided by the apparent rate constant of the same catalyst without nickel. These results are presented in Figs. 15 and 16.

Every catalyst exhibited increased hydroisomerization activity with the addition of nickel. One exception, however, was Ni-Be-M which had a lower activity than Be-M below 295°C. The increase in hydroisomerization activity followed the order Ba > Sr > Ca > Mg > Be. The increase in activity probably occurs because a mechanism change takes place with addition of nickel. One possible explanation is that the hydroisomerization mechanism changes from a Friedel-Crafts hydride extraction mechanism (*34,35*), typical of solid acid type catalysts (e.g., H-M), to a dual-function mechanism (*35,36*) where

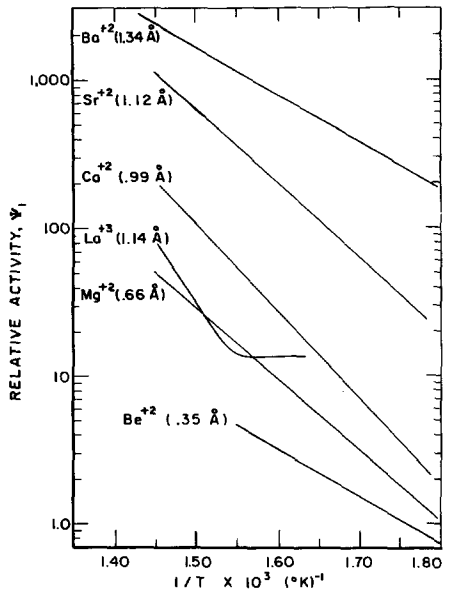

FIG. 15. Relative activity, ψ_1 vs inverse absolute temperature.

the transition metal sites can form an olefin intermediate. The larger cation mordenites are most likely capable of better conversions via a dual-function mechanism. The enhancement is not as great with a small cation like beryllium which has a much stronger polarizing field than the other alkaline earth cations and consequently can function almost as well via a Friedel–Crafts mechanism. Somewhat parallel to the above results, addition of a transition metal to Mg, Ca, Sr, and Ba Type Y zeolite catalysts greatly enhanced their *n*-hexane hydroisomerization activity (*30*), whereas addition of a transition metal to a solid acid type catalyst such as H–M did not enhance *n*-pentane hydroisomerization activity (*13*).

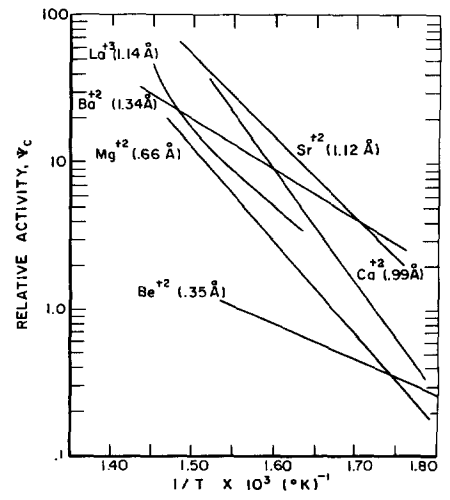

FIG. 16. Relative activity, Ψ_c vs inverse absolute temperature.

The hydrocracking mechanism on the nickel catalysts appears to be ionic in nature since the product distribution indicates splitting of pentane into either propane and ethane or butane and methane. As reaction temperature is increased some of these smaller fragments appear to be cracked further yielding more methane. A significant amount of the butane yield was isobutane. There is a possibility, however, that two cracking reactions are occurring simultaneously, one of which involves direct scission of a carbon–carbon bond and another which is a disproportionation reaction (*37*).

For the Be, Mg, and Ca catalysts, addition of nickel retarded the hydrocracking reaction below 370, 324, and 307°C, respectively, as shown in Fig. 16. For the Sr, Ba, and La catalysts hydrocracking activity was improved with the addition of nickel. The order of activity increase for the different cations was about the same as for hydroisomerization.

In comparing cracked product distribution, the catalysts which contained nickel consistently produced relatively more butanes and propane, and less methane than the same catalysts without nickel. Thus, the nickel appears to retard the formation of smaller fragments by changing the reaction mechanism. This retardation effect probably can be explained by the dual-function mechanism (*35,36*) where the transition metal regulates the carbonium ion concentration by olefin formation and hydrogenation. A change in reaction mechanism is evident because the activation energy increases significantly (Table 6). The activation energy for *n*-pentane hydroisomerization over a Pd–H–M catalyst

was reported to be about 30.6 to 38.0 kcal/g-mole (*13,19*). These values reasonably agree with those in Table 6.

As mentioned previously, the apparent reaction rate constants for Be–M and La–M behaved peculiarly with increased reaction temperature (Figs. 9 and 10). The addition of nickel to these catalysts eliminated the nonlinearity of the La–M catalyst Arrhenius plot completely, and delayed the change in the Be–M hydroisomerization activation energy to a temperature 28°C higher. The change in Be–M hydrocracking activation energy was apparently eliminated by addition of nickel. The behavior of these catalysts is not understood and will require further investigation. Diffusion limitation and deactivation from coking do not appear to be significant factors since the other catalysts showed no change in activation energy over the same temperature range nor a reduced activity over the integral time of the experiments. The product distributions for the Be–M and La–M catalysts indicate the production of methane and ethane increase rapidly with reaction temperature over the entire temperature range explored. However, the production of isopentane, butanes, and propane increases rapidly with increasing temperature below 370°C and increases much more slowly with increasing temperature above 310°C. Addition of nickel results in the butanes and propane yields increasing rapidly over the entire temperature range for both catalysts. Ni–Be–M exhibits a slow increase in isopentane yield at higher temperatures similar to Be–M whereas this effect is eliminated when nickel is added to La–M.

ACKNOWLEDGMENTS

This work would not have been possible without financial support through a N.D.E.A., Title IV Fellowship. Mr. William Ritter and Dr. Joseph Gianetti of Gulf Research and Development Company gave valuable advice during early stages of this project. Walter Marion, Olie Demeter, and Lawrence Herman gave considerable assistance in building the pilot unit.

REFERENCES

1. BENESI, H. A., *J. Catal.* **8,** 368 (1967).
2. HOPKINS, P. D., *J. Catal.* **12,** 325 (1968).
3. YASHIMA, T., MOSLEHI, H., AND HARA, N., *Bull. Jap. Petrol. Inst.* **12,** 106 (1970).
4. EBERLY, P. E., KIMBERLIN, C. N., AND VOORHIES, A. *J. Catal.* **22,** 419 (1971).
5. LEFRANCOIS, M., AND MALBOIS, G., *J. Catal.* **20,** 350 (1971).
6. YASHIMA, T., AND HARA, N., *J. Catal.* **27,** 329 (1972).
7. BECKER, K. A., KARGE, H. G., AND STREUBEL, W. D., *J. Catal.* **28,** 403 (1973).
8. BRYANT, D. E., AND KRANICH, W. L., *J. Catal.* **8,** 8 (1967).
9. CSICSERY, S. M., *J. Catal.* **19,** 394 (1970).
10. CSICSERY, S. M., *J. Catal.* **23,** 124 (1971).
11. MINACHEV, KH. M., GARANIN, V. I., KHARLAMOV, V. V., ISAKOVA, T. A., AND SENDEROV, E. E., *Proc. Acad. Sci. USSR Chem. Ser.* **8,** 1611 (1969).
12. MINACHEV, KH., GARANIN, V., ISAKOVA, I., KHALAMOV, V., AND BOGOMOLOV, V., "Advances in Chemistry," Series 102, p. 441. American Chemical Society, Washington, DC, 1971.
13. BRYANT, P. A., AND VOORHIES, A., *AIChE J.* **14,** 852 (1968).
14. BEECHER, R. G., AND VOORHIES, A., *Ind. Eng. Chem. Prod. Res. Dev.* **8,** 366 (1969).
15. BRYANT, P. A., Ph.D. Dissertation, Louisiana State University, 1966.
16. LANEWALA, M. A., PICKERT, P. E., AND BOLTON, A. P., *J. Catal.* **9,** 95 (1967).
17. GRAY, J. A., Ph.D. Dissertation, University of Pittsburgh, 1973.
18. MORRIS, A. G. C., *Analyst* **90,** 325 (1965).
19. HOPPER, J. R., AND VOORHIES, A., *Ind. Eng. Chem. Prod. Res. Dev.* **11,** 294 (1972).
20. BEECHER, R., VOORHIES, A., AND EBERLY, P., *Ind. Eng. Chem. Prod. Res. Dev.* **7,** 203 (1968).
21. LUZARRAGA, M. G., AND VOORHIES, A., *Ind. Eng. Chem. Prod. Res. Dev.* **12,** 194 (1973).
22. EVEREST, D. A., "The Chemistry of Beryllium." Vol. 1, p. 8, Amsterdam, Elsevier, 1964.
23. BALLIVET, D., PICHAT, P., AND BARTHOMEUF, D., "Advances in Chemistry," Series 121, p. 469, American Chemical Society, Washington, DC, 1973.
24. BOLTON, A. P., *J. Catal.* **22,** 9 (1971).
25. ALDRIDGE, L. P., MCLAUGHLIN, J. R., AND POPE, C. G., *J. Catal.* **30,** 409 (1973).
26. RABO, J. A., AND POUTSMA, M. L., "Advances in

Chemistry," Series 102, p. 284, American Chemical Society, Washington, DC, 1971.

27. HICKSON, D. A., AND CSICSERY, S. M., *J. Catal.* **10,** 27 (1968).
28. VENUTO, P. B., HAMILTON, L. A., LANDIS, P. S., AND WISE, J. J., *J. Catal.* **4,** 81 (1966).
29. BEAUMONT, R., BARTHOMEUF, D., AND TRAMBOUZE, Y., "Advances in Chemistry," Series 102, p. 327, American Chemical Society, Washington, DC, 1971.
30. PICKERT, P. E., RABO, J. A., DEMPSEY, E., AND SCHOMAKER, V., "Proceedings of the Third International Congress Catalysis," Vol. 1, p. 714, Amsterdam, North-Holland, 1964.
31. TSUTSUMI, K., AND TAKAHASHI, H., *J. Catal.* **24,** 1 (1972).
32. WARD, J. W., AND HANSFORD, R. C., *J. Catal.* **13,** 364 (1969).
33. SHARF, V. Z., *et al. Proc. Acad. Sci. USSR Chem. Ser.* **10,** 2076 (1971).
34. MINACHEV, KH. M., GARANIN, V. I., AND KHARLAMOV, V. V., *Proc. Acad. Sci. USSR Chem. Ser.* **4,** 785 (1970).
35. KOUWENHOVEN, H. W., AND VAN ZYLL LANGHART, W. C., *Chem. Eng. Prog.* **67,** 65 (1971).
36. WEISZ, P. B., *in* "Advances in Catalysis" (D. D. Eley, P. W. Selwood and P. B. Weisz, Eds.), Vol. 13, p. 137. New York, Academic Press, 1962.
37. BOLTON, A. P., AND BUJALSKI, R. L., *J. Catal.* **23,** 331 (1971).